Theoretical and Applied Climatology (2019) 135:1045–1058
https://doi.org/10.1007/s00704-018-2423-7

ORIGINAL PAPER

Comprehensive assessment of parameterization methods for estimating clear-sky surface downward longwave radiation

Yamin Guo[1] · Jie Cheng[1,2] · Shunlin Liang[1,2]

Received: 5 February 2017 / Accepted: 12 February 2018 / Published online: 26 February 2018

Abstract

Surface downward longwave radiation (SDLR) is a key variable for calculating the earth's surface radiation budget. In this study, we evaluated seven widely used clear-sky parameterization methods using ground measurements collected from 71 globally distributed fluxnet sites. The Bayesian model averaging (BMA) method was also introduced to obtain a multi-model ensemble estimate. As a whole, the parameterization method of Carmona et al. (2014) performs the best, with an average BIAS, RMSE, and R^2 of − 0.11 W/m^2, 20.35 W/m^2, and 0.92, respectively, followed by the parameterization methods of Idso (1981), Prata (Q J R Meteorol Soc 122:1127-1151, 1996), Brunt and Sc (Q J R Meteorol Soc 58:389-420, 1932), and Brutsaert (Water Resour Res 11:742-744, 1975). The accuracy of the BMA is close to that of the parameterization method of Carmona et al. (2014) and comparable to that of the parameterization method of Idso (1981). The advantage of the BMA is that it achieves balanced results compared to the integrated single parameterization methods. To fully assess the performance of the parameterization methods, the effects of climate type, land cover, and surface elevation were also investigated. The five parameterization methods and BMA all failed over land with the tropical climate type, with high water vapor, and had poor results over forest, wetland, and ice. These methods achieved better results over desert, bare land, cropland, and grass and had acceptable accuracies for sites at different elevations, except for the parameterization method of Carmona et al. (2014) over high elevation sites. Thus, a method that can be successfully applied everywhere does not exist.

1 Introduction

Surface downward longwave radiation (SDLR, 4–100 μm), which is mainly emitted by H_2O, CO_2, and O_3 molecules and cloud water droplets in the atmosphere near the earth's surface, is one of the four components required to calculate the earth's surface radiation budget (Idso and Jackson 1969; Duarte et al. 2006). Accurate estimates of SDLR are important for calculating surface net radiation, which determines the magnitude of the terms in the surface energy balance equation (e.g., soil heat flux, sensible heat flux, and latent heat flux) (Liang et al. 2010; Cheng and Liang 2016; Wang and Liang 2009a; Wang and Chen 2013).

The weighting function of SDLR peaks near the surface (Gupta et al. 2010; Schmetz 1989), so near surface temperature and/or water vapor are used to calculate SDLR based on the Stefan-Boltzmann equation.

$$\mathrm{SDLR} = \varepsilon(T_a, e_a)\sigma T_a^4 \tag{1}$$

where σ is the Stefan–Boltzmann constant (5.67 × 10–8 W m^{-2} K^{-4}). ε is the atmospheric effective emissivity under clear-sky conditions. ε can be modeled as a function of air temperature (T_a), water vapor pressure (e_a), or both. Different strategies of representing ε under clear-sky condition form various parameterization methods. Among these parameterization methods, some are empirically based while others have a solid physical basis. For example, Brunt (Brunt and Sc 1932) established the empirical relationship between SDLR and e_a based on a perceived similarity between heat conduction and radiative transfer. Three decades later, Swinbank (Swinbank

✉ Jie Cheng
brucechan2003@126.com

[1] State Key Laboratory of Remote Sensing Science, Jointly Sponsored by Beijing Normal University and Institute of Remote Sensing and Digital Earth of Chinese Academy of Sciences, Beijing Normal University, Beijing 100875, China

[2] Institute of Remote Sensing Science and Engineering, Faculty of Geographical Science, Beijing Normal University, Beijing 100875, China

1963) noted that SDLR is related to the square of T_a rather than e_a because precipitable water is more strongly correlated with screen temperature than with screen vapor pressure. Idso and Jackson (1969) theorized that the effective emittance of the atmosphere is a minimum at 273 K, and it increases symmetrically to exponentially approach unity at higher and lower temperatures. They developed a new formula that meets these standards and derived the coefficient of the formula using experimental data from Alaska, Arizona, Australia, and the Indian Ocean. In the methods of Swinbank (1963) and Idso and Jackson (1969), only air temperature is employed to estimate the atmospheric emissivity. Based on an analytic solution of Schwarzschild's equation for a nearly standard atmosphere, Brutsaert (1975) derived a more physical parameterization method. Using a standard temperature lapse rate, Marks and Dozier (1979) adjusted T_a and e_a at elevation z to the sea level equivalent and developed an elevation corrected model based on the method of Brutsaert (1975). Idso (1981) claimed that air emissivity should be nonlinearly dependent onT_a and e_a and derived a new formula using observations from Phoenix (AZ, USA), where the air temperature ranges from − 10 to 45 °C. Prata (1996) found that the method of Brutsaert (Brutsaert 1975) cannot correct for low water vapor amounts because the emissivity tends toward zero. He presented a new method by assuming that the absorption in the longwave spectrum can be represented by a simple exponential band model. Under cloudy conditions, the SDLR is increased because the liquid water and ice absorb and emit longwave radiation more effectively than water in the vapor phase. The parameterization methods for estimating cloudy-sky SDLR correct for clouds based on clear-sky SDLR. Therefore, accurate estimates for clear-sky SDLR are important for calculating cloudy-sky SDLR. Parameterization methods have been widely employed to estimated SDLR at global and regional scales. For example, Wang and Liang (Wang and Liang 2009b) estimated all-sky SDLR using meteorological observations from 1996 to 2007 at 36 globally distributed sites; Bisht and Bras (Bisht and Bras 2011) estimated the SDLR over the continental USA using the parameterization method of Prata (1996) from MODIS products.

We must be careful when selecting parameterization methods because most parameterization methods are site-specific, i.e., they were developed using a limited time span of data from a certain local area. Thus, they are affected by geographic location and local atmospheric conditions and cannot be applied elsewhere. Many studies have evaluated the performance of different parameterization methods, but most of them have been conducted for a certain region. Unfortunately, the derived conclusions are inconsistent and sometimes contradictory. Santos et al. 2011 tested the performance of nine clear-sky SDLR methods in the semiarid region of Northeast Brazil. Their study indicated that the parameterization method of Sugita and Brutsaert (Sugita and Brutsaert 1993) performed better than that of Brutsaert (Brutsaert 1975). However, the study of Duarte et al. (Duarte et al. 2006) in Southern Brazil found that the performance of the method of Brutsaert (Brutsaert 1975) is better than that of the method of Sugita and Brutsaert (Sugita and Brutsaert 1993). The parameterization method developed by Swinbank (Swinbank 1963) achieved the best results in the study of Kjaersgaard et al. (Kjaersgaard et al. 2007) that evaluated 11 parameterization methods using long time series measurements in Denmark, whereas the method of Swinbank (Swinbank 1963) performed the worst in the studies of Kruk et al. (Kruk et al. 2010) and Carmona et al. (2014). Rizou and Nnadi (Rizou and Nnadi 2007) noted that heterogeneous land cover types can affect atmospheric emissivity as well as air temperature and water vapor. Moreover, the derived coefficients of the same parameterization method are quite different if data from different areas are used. For example, nine different coefficients are reported for the widely used clear-sky parameterization method developed by Brunt (Brunt and Sc 1932), with the variability as large as 30% (Kjaersgaard et al. 2007).

The accuracy of the aforementioned parameterization methods at global and regional scales is unclear, and whether these methods can be applied to global or regional scales also remains unknown. The purpose of this study is to investigate the accuracy and applicability of widely used parameterization methods at global and regional scales, using ground observations collected from globally distributed flux measurement sites.

2 Data and method

2.1 Ground measurements

During the past two decades, several long-term ground observation networks deployed with pyrgeometers that measure SDLR have been established. Ground-measured SDLR and corresponding meteorological parameters (e.g., air temperature and relative humidity) collected from 71 globally distributed sites in 6 networks were used to evaluate the accuracy of typical parameterization methods. These sites include 29 sites from BSRN, 12 sites from AmeriFlux, 12 sites from Fluxnet, 8 sites from AsiaFlux, 6 sites from SurfRad, and 4 sites from CEOP. Figure 1 shows the spatial distribution of the sites. Table 1 summarizes the site information, including latitude, longitude, elevation, land cover, climate types, and the period of observation time. These sites are globally distributed and represent different climate and ecosystem conditions, ranging from the Arctic to the Antarctic. The land cover types of these sites include bare land, desert, cropland, grassland, forest, wetlands, and ice. The elevations of the sites range from 4 to 5038 m.

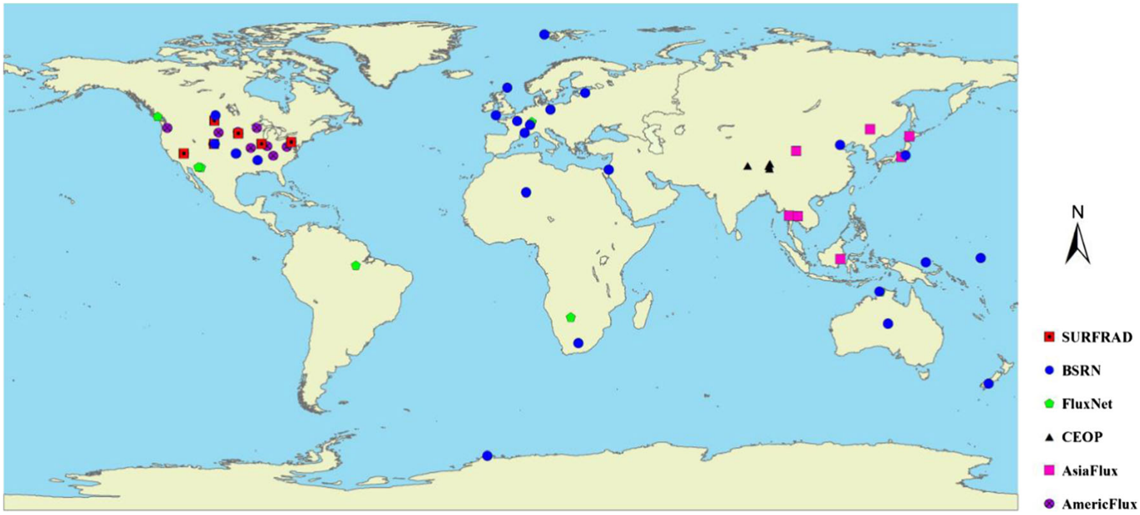

Fig. 1 Spatial distribution of 71 observation sites in 6 measurement networks

The clear sky was identified using a cloud fraction that was calculated using the following equation (Crawford and Duchon 1999):

$$c = 1 - \frac{SW_{\downarrow}}{SW_{\downarrow 0}} \tag{2}$$

where c is the cloud fraction, $SW_{\downarrow}$ is the ground measured surface incident shortwave radiation, and $SW_{\downarrow 0}$ is the theoretical shortwave clear-sky radiation calculated using the method of Carmona et al. (2014). The clear sky condition is identified when c is less than 0.05. Note that nighttime data were excluded because $SW_{\downarrow}$ was not available. The input parameter e_a (in hPa) was calculated by

$$e_a = e_s\left(\frac{RH}{100}\right) = \left(6.108\exp\left[\frac{17.27T_a}{T_a + 237.3}\right]\right)\left(\frac{RH}{100}\right) \tag{3}$$

where e_s (in hPa) is the saturation vapor pressure. T_a and relative humidity (RH) are in degrees centigrade and percentage, respectively. The derived clear-sky data for each site were randomly divided into two parts, two thirds for calibrating the coefficient and one third for evaluating the accuracy of the selected parameterization methods.

2.2 Methods

2.2.1 Clear-sky parameterization methods

Seven widely used parameterization methods were selected in this study. The parameterization methods take the form of Eq. (1) and are listed in Table 2. The first six parameterization methods were briefly described in Sect. 1. Carmona et al. (2014) established two multiple linear relationships between SDLR, T_a, and RH for all sky conditions using experimental data from a sub-humid region, Tandil, Argentina. The multiple linear relationships are expressed as shown below:

$$\mathrm{SDLR} = [(a + bT_a + dRH)(1-c) + c]\sigma T_a^4 \tag{4}$$

$$\mathrm{SDLR} = [e + fT_a + gRH + hc]\sigma T_a^4 \tag{5}$$

where a, b, d, e, f, g, and h are locally calibrated constants, and c is the cloud fraction. In clear sky conditions, c is equal to zero. Substituting $c = 0$ into Eqs. (4) and (5), we obtained a new formula,

$$\mathrm{SDLR} = [a_7 + b_7T_a + d_7RH]\sigma T_a^4 \tag{6}$$

2.2.2 Bayesian model averaging method

Bayesian model averaging (BMA) is a standard method for combining predictive distributions from different sources (Hoeting et al. 1999). The BMA predictive probability density function (PDF) is a weighted average of the forecast distributions from each model separately. The weight is given by the posterior probability of each model, which reflects the models' predictive performance. (Raftery et al. 2003).

BMA was used to obtain a more accurate estimate of SDLR by combining the results obtained from the parameterization methods. For convenience, we employ r and R to represent the predictive and corresponding in situ SDLR, respectively, at a given time. $\{f_1, f_2, f_3 \ldots, f_n\}$is an ensemble of n models that predict r. According to the total

Table 1 Description of ground sites used in this study

No.	Short name	Full name	Latitude	Longitude	Elevation (m)	Land cover	Climate type[g]	Temporal resolution	Time period
1	Bondville[a]	Bondville, Illinois	40.05	− 88.37	213	Cropland	Dfa	3 min	2003–2005
2	Boulder[a]	Boulder, Colorado	40.13	− 105.24	1689	Grassland	BSk	3 min	2003–2005
3	Fort Peck[a]	Fort Peck, Montana	48.31	− 105.10	634	Grassland	BSk	3 min	2003–2005
4	Desert Rock[a]	Desert Rock, Nevada	36.63	− 116.02	1007	Desert	BWh	3 min	2003–2005
5	Penn State[a]	Penn State, Pennsylvania	40.72	− 77.93	376	Cropland	Dfb	3 min	2003–2005
6	Sioux Falls[a]	Sioux Falls, South Dakota	43.73	− 96.62	473	Cropland	Dfa	3 min	2003–2005
7	US-Blk[b]	Black Hills	44.16	− 103.65	1718	Evergreen needle leaf forest	Dfb	30 min	2004–2006
8	US-Bo2[b]	Bondville (companion site)	40.01	− 88.29	219.3	Cropland	Dfa	30 min	2004–2006
9	US-Bkg[b]	Brookings	44.35	− 96.84	510	Grasslands	Dfa	30 min	2004–2006
10	US-CaV[b]	Canaan Valley	39.06	− 79.42	994	Grasslands	Cfb	30 min	2004–2006
11	US-NR1[b]	Niwot Ridge Forest	40.03	− 105.55	3050	Evergreen needle leaf forest	Dfc	30 min	2001–2003
12	US-FPe[b]	Fort Peck	48.31	− 105.1	634	Grassland	Bsk	30 min	2003–2005
13	US-Goo[b]	Goodwin Creek	34.25	− 89.87	87	Grasslands	Cfa	30 min	2003–2005
14	US-MMS[b]	Morgan Monroe State Forest	39.32	− 86.41	275	Deciduous broadleaf forest	Cfa	30 min	2001–2003
15	US-WBW[b]	Walker Branch Watershed	35.96	− 84.29	283	Deciduous broadleaf forest	Cfa	30 min	2003–2005
16	US-Wrc[b]	Wind River Crane Site	45.82	− 121.95	371	Evergreen needleleaf forest	Csb	30 min	2003–2005
17	US-WCr[b]	Willow Creek	45.81	− 90.08	520	Deciduous broadleaf forest	Dfb	30 min	2003–2005
18	US-MOz[b]	Missouri Ozark Site	38.74	− 92.20	220	Deciduous broadleaf forest	Cfa	30 min	2003–2005
19	QHB[c]	Qinghai Flux Research Site	37.61	101.33	3250	Grasslands	BSk	15 min	2003–2004
20	MKL[c]	Mae Klong	14.58	98.84	231	Mix forest	Am	15 min	2003–2004
21	TKY[c]	Takayama	36.15	137.42	1420	Deciduous broadleaf forest	Dfb	15 min	2003–2005
22	TMK[c]	Tomakomai Flux Research Site	42.74	141.52	140	Deciduous needle leaf forest	Dfb	15 min	2001–2003
23	BKS[c]	Bukit Soeharto	− 0.86	117.04	20	Evergreen broadleaf forest	Af	15 min	2001–2002
24	FJY[c]	Fujiyoshida	35.45	138.76	1030	Deciduous needleleaf forest	Cfa	15 min	2000
25	LSH[c]	Laoshan	45.28	127.58	340	Deciduous needleleaf forest	Cfc	15 min	2002
26	SKR[c]	Sakaerat	14.49	101.92	543	Evergreen broadleaf forest	Aw	15 min	2001–2003
27	Amdo[d]	Amdo Tower	32.24	91.62	4695	Bare land	ET	60 min	2002–2004
28	BJ[d]	BJ Tower	31.37	91.90	4509	Bare land	ET	60 min	2002–2004
29	D105[d]	D105-AWS	33.06	91.94	5038	Bare land	ET	60 min	2002–2004
30	Gaize[d]	Gaize	32.30	84.05	4416	Bare land	Dwb	60 min	2002–2004
31	BOU[e]	Boulder	40.05	− 105.01	1577	Grasslands	BSk	1 min	2003–2005
32	CAR[e]	Carpentras	44.08	5.06	100	Cultivated	Csb	1 min	2003–2005
33	DAR[e]	Darwin	− 12.43	130.89	30	Grasslands	Aw	1 min	2003–2005
34	LIN[e]	Lindenberg	52.21	14.12	125	Cultivated	Dfb	1 min	2003–2005
35	MAN[e]	Momote	− 2.06	147.43	6	Grasslands	Af	1 min	2003–2005
36	NAU[e]	Nauru Island	− 0.52	166.92	7	Rock	Af	1 min	2003–2005
37	NYA[e]	Ny-Ålesund	78.93	11.93	141	Tundra	ET	1 min	2003–2005
38	PAY[e]	Payerne	46.82	6.94	491	Cultivated	Dfb	1 min	2003–2005
39	REG[e]	Regina	50.21	− 104.71	578	Cultivated	Dfb	1 min	2003–2005
40	E13[e]	Southern Great Plains	36.61	− 97.49	318	Grasslands	Cfa	5 min	2003–2005
41	TAT[e]	Tateno	36.05	140.13	25	Grasslands	Cfa	1 min	2003–2005
42	DAA[e]	De Aar	− 30.7	23.99	1287	Desert	BWk	5 min	2002–2004
43	GVN[e]	Georg von Neumayer	− 70.65	− 8.25	42	Ice	EF	1 min	2003–2005
44	SBO[e]	Sde Boqer	30.86	34.78	500	Desert	BWk	1 min	2003–2005
45	ASP[e]	Alice Springs	− 23.80	133.89	547	Grasslands	BWh	1 min	2003–2005

Table 1 (continued)

No.	Short name	Full name	Latitude	Longitude	Elevation (m)	Land cover	Climate type[g]	Temporal resolution	Time period
46	BIL[e]	Billings	36.61	− 97.52	317	Grasslands	Cfa	1 min	2003–2005
47	BON[e]	Bondville	40.07	− 88.37	213	Grasslands	Dfa	3 min	2003–2005
48	BOS[e]	Boulder	40.125	− 105.24	1689	Grasslands	Dfa	3 min	2003–2005
49	CAM[e]	Camborne	50.22	− 5.32	88	Grasslands	Cfb	1 min	2003–2005
50	DRA[e]	Desert Rock	36.63	− 116.02	1007	Desert	BWh	3 min	2003–2005
51	GCR[e]	Goodwin Creek	34.25	− 89.87	98	Grasslands	Cfa	3 min	2003–2005
52	LAU[e]	Lauder	− 45.045	169.689	350	Grass	Cfb		2003–2005
53	LER[e]	Lerwick	60.14	− 1.18	80	Grasslands	Cfb	1 min	2003–2005
54	PAL[e]	Palaiseau, SIRTA Observatory	48.71	2.21	156	Concrete	Cfb	1 min	2006
55	PSU[e]	Rock Springs	40.72	− 77.93	376	Cultivated	Dfa	3 min	2003–2005
56	SXF[e]	Sioux Falls	43.73	− 96.62	473	Grasslands	Dfa	3 min	2004–2006
57	TAM[e]	Tamanrasset	22.79	5.52	1385	Desert	BWh	1 min	2003–2005
58	TOR[e]	Toravere	58.25	26.46	70	Grasslands	Dfb	1 min	2003–2005
59	XIA[e]	Xianghe	39.75	116.96	32	Desert	Dwa	1 min	2005–2007
60	AU-How[f]	Howard Springs	− 12.50	131.20	41	Savanna	Aw	30 min	2003–2005
61	BW-GhG[f]	Ghanzi Grass Site	− 21.50	21.74	1161	Grassland	BSh	30 min	2003
62	BW-GhM[f]	Ghanzi Mixed Site	− 21.20	21.75	1139	Savannas	BSh	30 min	2003
63	CA-Ca1[f]	BC-Campbell River 1949 Douglas-fir	49.87	− 125.30	313	Evergreen Needleleaf Forest	Csb	30 min	2003–2005
64	CN-Do1[f]	Dongtan 1	31.52	121.96	6	Wetlands	Cfa	30 min	2005
65	CN-Do2[f]	Dongtan 2	31.58	121.90	4	Woody Savannas	Cfa	30 min	2005
66	CN-Do3[f]	Dongtan 3	31.52	121.97	6	Wetlands	Cfa	30 min	2005
67	DE-Har[f]	Hartheim	47.93	7.60	201	Mixed forests	Cfb	30 min	2005–2006
68	US-Wkg[f]	Walnut Gulch Kendall Grasslands	31.74	− 109.94	1524	Grasslands	BSk	30 min	2004–2006
69	US-SRM[f]	Santa Rita Mesquite	31.82	− 110.87	1118	Open shrublands	BSk	30 min	2004–2006
70	BR-Sa3[f]	Santarem-Km83-Logged Forest	− 3.02	− 54.97	100	Evergreen Broadleaf Forest	Am	30 min	2001–2003
71	BW-MA1[f]	Maun-Mopane Woodland	− 19.92	23.56	950	Savannas	Bsh	30 min	2000–2001

[a] SurfRad

[b] AmeriFlux

[c] AsiaFlux

[d] CEOP

[e] BSRN

[f] Fluxnet

[g] Koppen climate classification (https://en.wikipedia.org/wiki/K%C3%B6ppen_climate_classification)

Table 2 Clear-sky parameterization methods evaluated in this study

Parameterization methods	Formula
Brunt and Sc (1932)	$\mathrm{SDLR} = \left(a_1 + b_1 e_a^{1/2}\right) \sigma T_a^4$
Swinbank (1963)	$\mathrm{SDLR} = \left(a_2 T_a^2\right) \sigma T_a^4$
Idso and Jackson (1969)	$\mathrm{SDLR} = (1 - a_3 \exp[\mathrm{b}_3 (273 - \mathrm{T}_a)^{2}]) \sigma T_a^4$
Brutsaert (1975)	$\mathrm{SDLR} = \left(a_4 \left(\frac{e_a}{T_a}\right)^{b4}\right) \sigma T_a^4$
Idso (1981)	$\mathrm{SDLR} = \left(a_5 + b_5 e_a \exp\left[\frac{1500}{T_a}\right]\right) \sigma T_a^4$
Prata (1996)	$\mathrm{SDLR} = \left(1 - \left[\left(1 + 46.5\left(\frac{e_a}{T_a}\right)\right) \exp\left(-\left(a_6 + b_6 46.5\left(\frac{e_a}{T_a}\right)\right)^{\frac{e_a}{T_a}}\right)\right]\right) \sigma T_a^4$
Carmona et al. (2014)	$\mathrm{SDLR} = (a_7 + b_7 T_a + d_7 R\mathrm{h}) \sigma T_a^4$

probability formula, the predictive PDF of r based on the multi model ensemble is given by

$$p(r|f_1, f_2 \ldots, f_n) = \sum_{i=1}^{n} p(r|f_i) p(f_i|R) \tag{7}$$

where $p(r|f_i)$ is the forecast PDF based on f_i alone and $p(f_i|R)$ is the posterior probability of f_i being correct given the measurement, which can reflect how well the model f_i fits the observed data. The posterior probabilities of all the single models add up to one, so $\sum_{i=1}^{n} p(f_i|R) = 1$. Thus, they can be viewed as weights, w_i. Equation (7) can be rearranged as follows:

$$p(r|f_1, f_2 \ldots, f_n) = \sum_{i=1}^{n} w_i p(r|f_i) \tag{8}$$

Assuming that the conditional PDF of r is normally distributed, it can be defined by the expected value, E, and variance, σ^2, with $g(\bullet)$ representing the associated Gaussian PDF.

$$p(r|f_i) = g\left(r|\left\{E_i, \sigma_i^2\right\}\right) \tag{9}$$

$$p(r|f_1, f_2 \ldots, f_n) = \sum_{i=1}^{n} w_i g\left(r|\left\{E_i, \sigma_i^2\right\}\right) \tag{10}$$

The optimal estimation of SDLR by BMA is the conditional expected value of r, and can be expressed as follows:

$$Exp(r|f_1, f_2 \ldots, f_n) = \sum_{i=1}^{n} w_i E_i \tag{11}$$

Thus, the key problem is obtaining the posterior probabilities of each model w_i, which renders the estimated SDLR closest to the measurement R. On the basis of Bayesian theory, we can get the best prediction when the likelihood function Eq. (10) is maximized. The logarithm of the likelihood function is used for convenience. We use the expectation-maximization algorithm to maximize the likelihood function.

3 Results and discussion

3.1 Adjusted coefficients and validation

First, we evaluated seven parameterization methods with their original coefficients. Then, the coefficients were calibrated by using two thirds of the samples from all sites. The remaining one third of the samples were used to test

Table 3 Comparison of original and adjusted coefficient values for seven clear-sky parameterization methods

Parameterization methods	Coefficients	Adjusted coefficients	Original coefficients	Relative difference (%)
Brunt and Sc (1932)	a_1	0.6338	0.52	21.88
	b_1	0.0426	0.065	− 34.46
Swinbank (1963)	a_2	9.0059×10^{-6}	9.365×10^{-6}	− 3.83
Idso and Jackson (1969)	a_3	0.2561	0.261	− 1.88
	b_3	-2.9006×10^{-4}	-7.77×10^{-4}	− 62.67
Brutsaert (1975)	a_4	1.0456	1.24	− 15.68
	b_4	0.0879	1/7	− 38.53
Idso (1981)	a_5	0.6836	0.7	− 2.34
	b_5	4.6869×10^{-5}	5.95×10^{-5}	− 21.23
Prata (1996)	a_6	1.3471	1.2	12.26
	b_6	2.7735	3	− 7.55
Carmona et al. (2014)	a_7	− 0.4373	− 0.34	28.62
	b_7	0.0037	0.00336	10.12
	d_7	0.0027	0.00194	39.18

the performance of the parameterization methods. The BIAS and RMSE were used as the primary indicators of the accuracy. The BIAS is given by

$$\mathrm{BIAS} = \frac{1}{n}\sum_{i=1}^{n}\left[\mathrm{SDLR}_{p,i} - \mathrm{SDLR}_{o,i}\right] \quad (12)$$

where $\mathrm{SDLR}_{p,\ i}$ and $\mathrm{SDLR}_{o,\ i}$ are the predicted and observed values, respectively. n is the number of samples. The root mean square error (RMSE) is given by

$$\mathrm{RMSE} = \sqrt{\frac{1}{n-1}\sum_{i=1}^{n}\left[\mathrm{SDLR}_{p,i} - \mathrm{SDLR}_{o,i}\right]^2} \quad (13)$$

In addition to BIAS and RMSE, the determination coefficient (R^2) was also used as an indicator to test the performance of the parameterization methods. The original and adjusted coefficient values are shown in Table 3. Overall, the adjusted coefficient values were significantly different from the original values, and with the exception of the parameterization methods of Swinbank (Swinbank 1963) and Prata (1996), their relative differences were less than 15%. Thus, it is highly important for real applications to adjust the coefficients using more realistic data.

Figure 2 shows the accuracy of the parameterization methods. Clearly, the accuracy of all the methods using the adjusted coefficients is greatly improved. As shown in Table 4, the BIAS of the adjusted coefficients ranges from − 4.53 to 0.01 W/m^2, whereas the BIAS of the original coefficients lies between − 16.96 and 15.99 W/m^2. The RMSE of the adjusted coefficients ranges from 20.35 to 34.38 W/m^2, whereas the RMSE of the original coefficients lies between 22.23 and 36.65 W/m^2. R^2 almost does not change. The SDLR is underestimated by the methods using adjusted coefficients, except for the parameterization method of Idso and Jackson (1969). The RMSEs of the parameterization methods of Swinband (1963) and Idso and Jackson (1969) are obviously larger than those of the other methods, and the R^2 values of these two methods are clearly lower than those of the other methods. Because e_a is not considered in the parameterization methods of Swinbank (1963) and Idso and Jackson (1969), their accuracy is worse than the other parameterization methods. This is in agreement with previous studies (Duarte et al. 2006; Kjaersgaard et al. 2007; Kruk et al. 2010; Carmona et al. 2014). Regarding the remaining five parameterization methods, the parameterization method of Carmona et al (2014) performs best, whose BIAS, RMSE, and R^2 are − 0.11 W/m^2, 20.35 W/m^2, and 0.92, respectively, followed by the parameterization methods of Idso (1981), Prata (1996), Brunt and Sc (1932), and Brutsaert (1975).

We also combined five relatively accurate parameterization methods (Brunt and Sc (1932), Brutsaert (1975), Idso (1981), Prata (1996), and Carmon (2014)) using

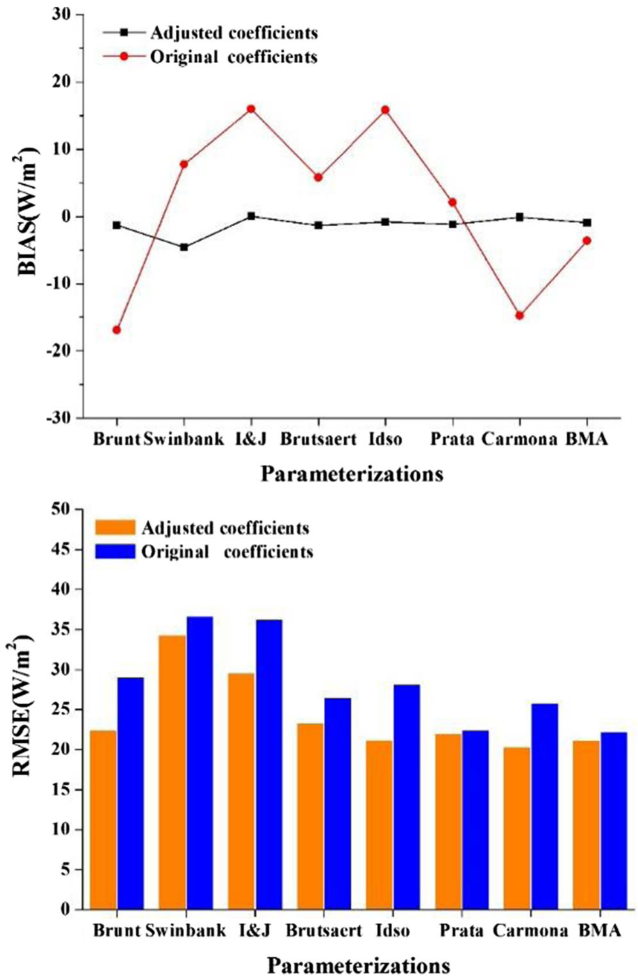

Fig. 2 The accuracy of seven parameterization methods as well as BMA

BMA to obtain multi-model ensemble estimates. The accuracy of the BMA is close to that of the parameterization method of Carmona et al. (2014) and comparable to that of the parameterization method of Idso (1981). Checking

Table 4 Statistical results of seven parameterization models and BMA using original and adjusted coefficients

Parameterizations	Adjusted coefficients			Original coefficients		
	BIAS	RMSE	R^2	BIAS	RMSE	R^2
Brunt and Sc (1932)	− 1.27	22.41	0.91	− 16.96	29.05	0.91
Swinbank (1963)	− 4.53	34.38	0.83	7.72	36.65	0.83
Idso and Jackson (1969)	0.01	29.62	0.81	15.99	36.31	0.83
Brutsaert (1975)	− 1.36	23.35	0.9	5.77	26.5	0.91
Idso (1981)	− 0.79	21.21	0.92	15.82	28.19	0.92
Prata (1996)	− 1.13	21.96	0.91	2.05	22.41	0.92
Carmona et al. (2014)	− 0.11	20.35	0.92	− 14.81	25.85	0.91
BMA	− 0.89	21.13	0.92	− 3.60	22.23	0.92

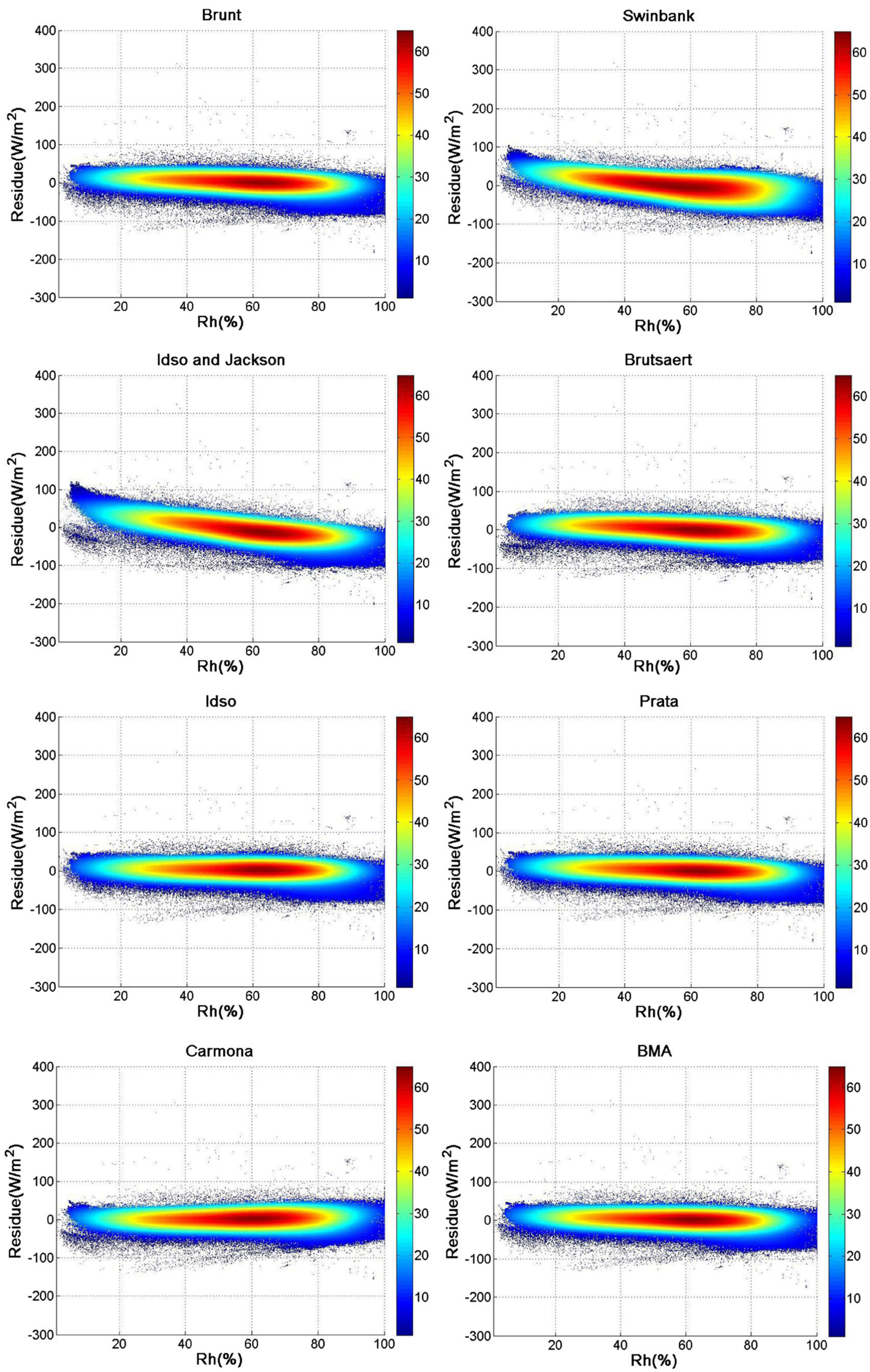

Fig. 3 Relative humidity sensitivity of seven parameterization methods and BMA

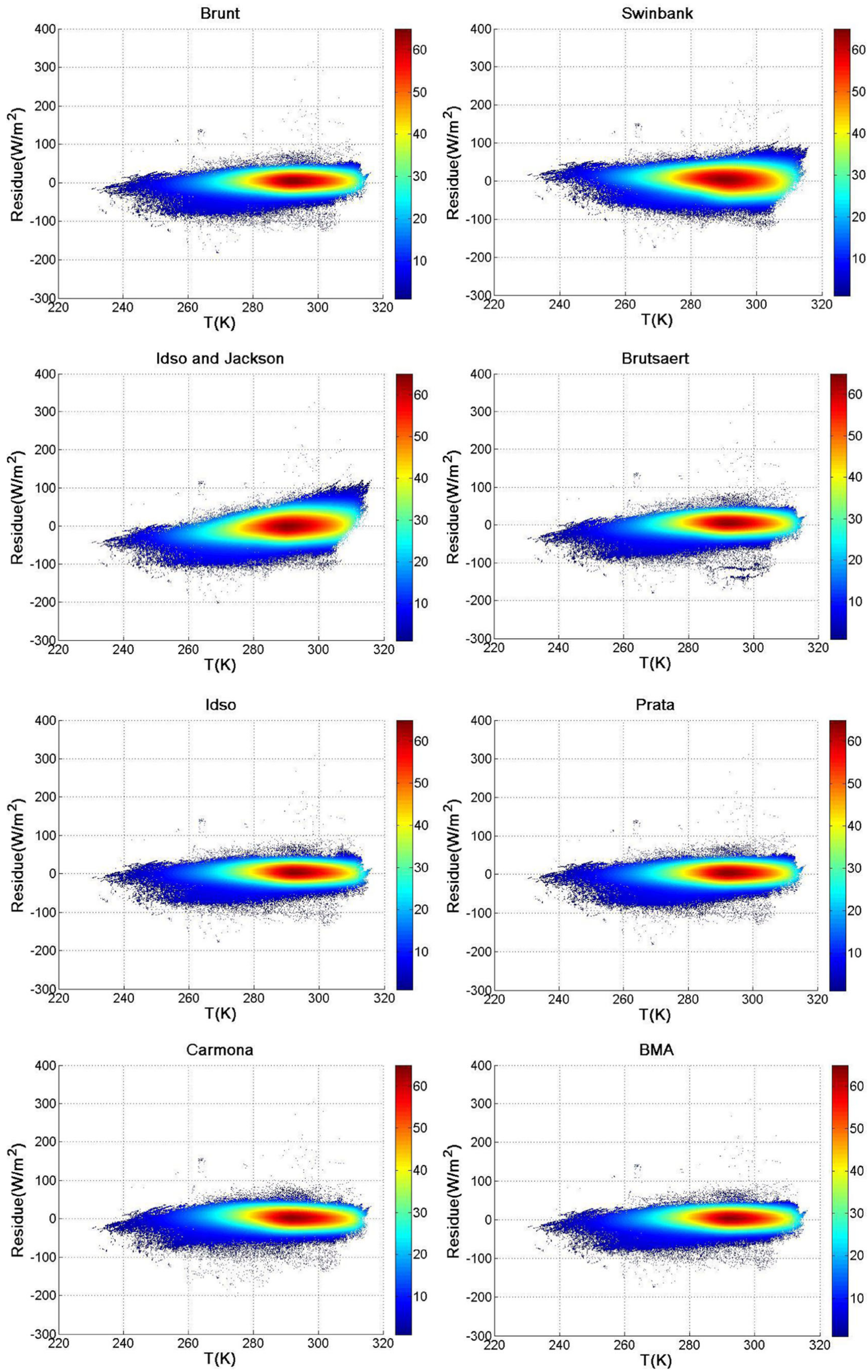

Fig. 4 Air temperature sensitivity of seven parameterization methods and BMA

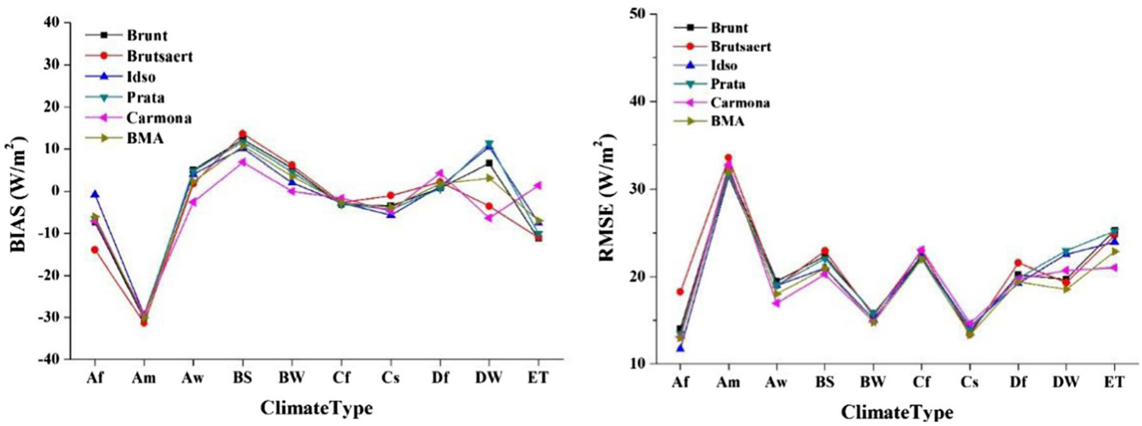

Fig. 5 Performance of five parameterization methods and BMA over different climate types

the results from each site, we found that the BMA achieves balanced results, that is, the accuracy is neither the best nor the worst when compared to the results of the five integrated parameterization methods.

Figures 3 and 4 show the scatterplot of residuals versus relative humidity and air temperature, respectively. Generally, the variation of residues with respect to relative humidity and air temperature is not significant, except for the parameterization methods of Swinbank (1963) and Idso and Jackson (1969). The residuals of these two parameterization methods decrease with relative humidity and increase with air temperature. When the air temperature is higher than 310 K, SDLR is overestimated by the parameterization methods of Swinbank (1963) and Idso and Jackson (1969).

To fully assess the parameterization methods, the sites were divided into different types according to climate type, land cover, and surface elevation. Due to their poor performance, the parameterization methods of Swinbank (1963) and Idso and Jackson (1969) were not considered in the following analysis.

Table 5 Statistical results of five parameterization models and BMA over different climate types

Climate type	BIAS						RMSE			
	Brunt	Brutsaert	Idso	Prata	Carmona	BMA	Brunt	Brutsaert	Idso	Prata
Af	− 7.43	− 13.96	− 0.80	− 6.48	− 7.10	− 6.08	14.01	18.24	11.68	13.46
Am	− 30.32	− 31.32	− 29.41	− 29.89	− 29.27	− 30.02	32.18	33.57	31.48	31.70
Aw	5.06	1.74	4.07	4.81	− 2.59	2.33	19.49	18.93	19.01	19.03
BS	12.20	13.52	10.12	11.61	6.88	10.67	22.32	22.90	21.01	22.04
BW	5.38	6.13	1.99	4.59	− 0.07	3.51	15.80	15.49	15.14	15.79
Cf	− 3.20	− 2.75	− 2.82	− 3.15	− 1.72	− 2.74	22.25	22.93	22.15	22.07
Cs	− 3.47	− 1.05	− 5.69	− 4.36	− 4.81	− 3.79	13.78	13.36	14.27	13.92
Df	0.73	2.22	1.10	0.65	4.29	1.79	20.23	21.55	19.28	19.86
DW	6.65	− 3.59	10.52	11.32	− 6.35	3.13	19.72	19.33	22.52	22.92
ET	− 11.22	− 10.98	− 7.49	− 10.06	1.35	− 6.99	25.27	24.66	23.91	25.21

Climate type	RMSE		R^2					
	Carmona	BMA	Brunt	Brutsaert	Idso	Prata	Carmona	BMA
Af	13.10	12.98	0.05	0.04	0.08	0.05	0.09	0.07
Am	32.77	32.04	0.82	0.75	0.79	0.83	0.49	0.79
Aw	16.96	18.00	0.56	0.41	0.66	0.59	0.65	0.60
BS	20.29	20.97	0.85	0.86	0.83	0.84	0.84	0.85
BW	14.85	14.74	0.87	0.88	0.84	0.86	0.87	0.87
Cf	23.04	21.98	0.87	0.86	0.87	0.88	0.85	0.87
Cs	14.64	13.35	0.92	0.92	0.92	0.92	0.90	0.92
Df	19.73	19.42	0.87	0.86	0.88	0.88	0.87	0.88
DW	20.73	18.58	0.84	0.88	0.78	0.78	0.87	0.86
ET	21.03	22.84	0.53	0.63	0.48	0.45	0.68	0.59

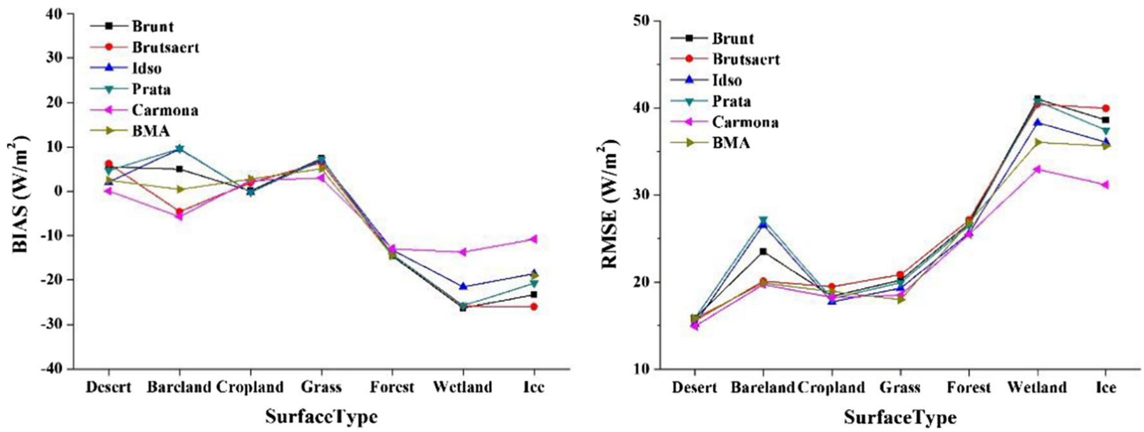

Fig. 6 Performance of five parameterization methods and BMA over different land cover types

3.2 Effects of climate type

Based on the Koppen climate classification, we divided the sites into 10 groups using their geolocations: Af (tropical rainforest climate), Am (tropical monsoon climate), Aw (tropical wet and dry or savanna climate), BS (semiarid), BW (desert climate), Cf (temperate or subtropical hot summer climates), Cs (mediterranean climates), Df (warm summer continental climates), Dw (dry winter continental climates), and ET (tundra climate). We then evaluated the selected parameterization methods over different climate types.

Figure 5 shows the evaluation results over ten climate types, and the statistical results are provided in Table 5. SLDR is highly underestimated by all methods over Am, with a BIAS around − 30 W/m^2 and RMSE larger than 30 W/m^2. SDLR is also underestimated by all methods over Af. SLDR is overestimated over the BS and BW climate types, with the exception of the parameterization method of Carmona et al. (2014) over BW. These results indicated that SLDR is prone to be underestimated when water vapor is high and overestimated when water vapor is low. Regarding the underestimation, there are two possible reasons: (1) the parameterization methods do not work well under high water vapor circumstances, and (2) the data derived from the tropical climate type in this study are not widely representative. There are only two sites (MKL and Sa3) in Am and three sites (BKS, MAN, and NAU) in Af. Flerchinger et al. (Flerchinger et al. 2009) noted that estimates of clear-sky SDLR were most

Table 6 Statistical results of five parameterization models and BMA over different land cover

Surface type	BIAS						RMSE			
	Brunt	Brutsaert	Idso	Prata	Carmona	BMA	Brunt	Brutsaert	Idso	Prata
Desert	5.43	6.17	2.04	4.63	− 0.02	3.56	15.86	15.56	15.21	15.85
Bare land	4.97	− 4.65	9.49	9.61	− 5.73	0.88	23.52	20.12	26.62	27.18
Cropland	0.10	1.86	− 0.26	− 0.22	2.39	0.74	18.40	19.49	17.75	18.12
Grass	7.39	6.42	7.05	7.14	2.97	6.09	20.25	20.88	19.29	19.94
Forest	− 14.56	− 14.24	− 13.26	− 14.19	− 12.94	− 13.81	26.77	27.14	25.64	26.52
Wetland	− 26.32	− 25.92	− 21.52	− 25.75	− 13.72	− 21.73	41.04	40.43	38.35	40.78
Ice	− 23.30	− 26.07	− 18.60	− 20.71	− 10.78	− 18.94	38.62	39.97	36.07	37.44

Surface type	RMSE		R^2					
	Carmona	BMA	Brunt	Brutsaert	Idso	Prata	Carmona	BMA
Desert	14.93	14.81	0.87	0.88	0.84	0.86	0.87	0.87
Bare land	19.74	20.63	0.53	0.63	0.48	0.45	0.68	0.70
Cropland	18.26	17.71	0.89	0.88	0.89	0.89	0.88	0.89
Grass	18.50	19.04	0.91	0.90	0.92	0.91	0.92	0.92
Forest	25.52	25.84	0.88	0.87	0.88	0.88	0.89	0.89
Wetland	32.94	37.70	0.75	0.74	0.76	0.75	0.77	0.76
Ice	31.18	35.61	0.53	0.54	0.53	0.53	0.57	0.55

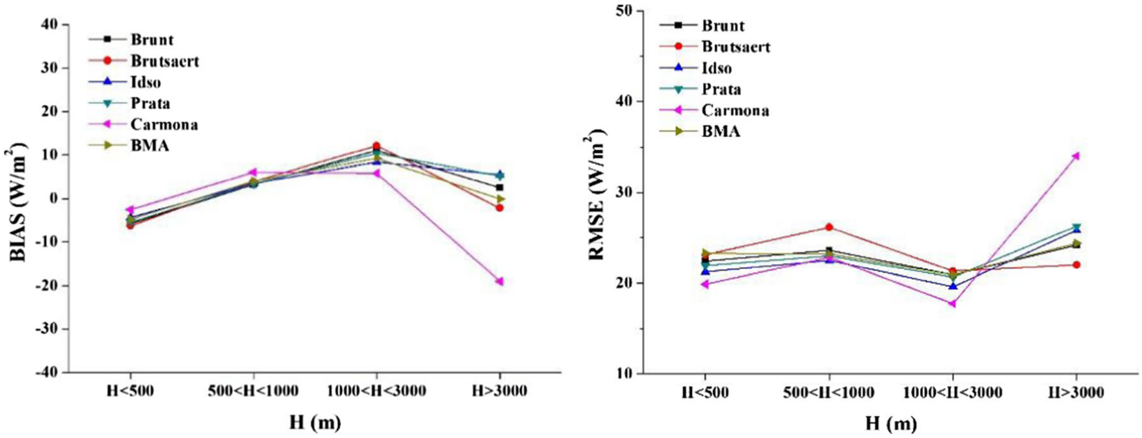

Fig. 7 Performance of five parameterization methods and BMA over different surface elevations

accurate in sites with the most number of clear days. Also, the sites with a low probability of clear conditions have low prediction accuracy. Tropical climates (Af and Am) have year-round high temperatures and are rainy, with a low probability of clear conditions, meaning that they are more likely affected by clouds. The influence of cloud contamination may contribute to the low estimation accuracy. As noted by Gupta et al. (Gupta et al. 2010), the overestimation of SDLR over dry-arid regions is a result of excessive heating of the surface during times of high surface insolation. Without considering the results at Am, the differences between the remaining climate types are not significant. Overall, the average BIAS for the six parameterization methods ranges from − 4.00 to − 1.84 W/m^2, the RMSE is less than 21.07 W/m^2, and the average R^2 is larger than 0.70. The parameterization method of Idso and Jackson (1969) has the lowest BIAS and seems better than other methods. The average BIAS, RMSE, and R^2 values are − 1.84 W/m^2, 20.05 W/m^2, and 0.71, respectively.

3.3 Effects of land cover

To analyze the effects of land cover on the performances of the selected parameterization methods, we divided the sites into seven groups: desert, bare land, cropland, grass, forest, wetland, and ice. The performance of each parameterization method over each type of land cover is shown in Fig. 6 and Table 6. All methods achieve better results over desert, bare land, cropland, and grass, but decline greatly over forest, wetland, and ice. The average BIAS of all methods over desert, bare land, cropland, and grass range from − 0.10 to 5.29 W/m^2, whereas the BIAS over forest, wetland, and ice is quite high and ranges from − 22.08 to − 12.48 W/m^2; the corresponding RMSE of the former four types of land cover is significantly lower than the latter three; the R^2 of the former four types of land cover is slightly higher than the latter three. The parameterization method of Carmona et al (2014) has the lowest RMSE, highest R^2, and second lowest BIAS, and the corresponding average values are 23.01 W/m^2, 0.80, and −

Table 7 Statistical results of five parameterization models and BMA over different elevations

Elevation	BIAS						RMSE			
	Brunt	Brutsaert	Idso	Prata	Carmona	BMA	Brunt	Brutsaert	Idso	Prata
H < 500	− 5.77	− 6.27	− 4.32	− 5.43	− 2.56	− 4.73	22.41	23.11	21.23	21.95
500 < H < 1000	3.28	3.97	3.53	3.41	6.07	4.07	23.61	26.16	22.49	23.01
1000 < H < 3000	11.07	12.14	8.38	10.38	5.86	9.26	20.93	21.31	19.60	20.66
H > 3000	2.49	− 2.18	5.47	5.21	− 19.03	− 0.10	24.20	22.01	25.80	26.27

Elevation	RMSE		R^2					
	Carmona	BMA	Brunt	Brutsaert	Idso	Prata	Carmona	BMA
H < 500	19.92	21.02	0.93	0.93	0.94	0.93	0.94	0.94
500 < H < 1000	22.82	22.80	0.87	0.85	0.87	0.87	0.86	0.87
1000 < H < 3000	17.75	19.38	0.85	0.86	0.82	0.83	0.86	0.85
H > 3000	34.00	23.24	0.61	0.77	0.49	0.48	0.61	0.66

5.40 W/m^2, respectively. The BMA has a balanced result over each land cover type.

3.4 Effects of surface elevation

Similar to the analytical approach for the effects of climate type and land cover type, we divided the site surface elevations (H, in m) into four ranges, H < 500, 500 < H < 1000, 1000 < H < 3000, and 3000 < H, to assess the effects of surface elevation. The assessment results are shown in Fig. 7. The differences among the parameterization methods are small over the four elevation ranges with the exception of Carmona et al. (2014) at high elevation sites, whose BIAS and RMSE are the largest over high elevation sites. The BIAS of each parameterization method over the low elevation sites is better than that for the high elevation sites. As shown in Table 7, among the different parameterization methods, the parameterization method of Brutsaert (1975) has the highest R^2 and lowest BIAS, and the corresponding average values are 0.85 and 1.92 W/m^2, respectively. The BMA has the lowest RMSE at 21.61 W/m^2.

4 Conclusion

SDLR is a key variable for calculating the surface radiation budget. The accuracy and applicability of seven widely used parameterization methods for estimating clear-sky SDLR at global and regional scales were investigated using ground measurements collected from 71 globally distributed fluxnet sites. The Bayesian averaging method was also applied to integrate the estimates of a multi-model ensemble for more reliable SDLR estimates. The following conclusions can be drawn:

1. The accuracies of the seven parameterization methods using adjusted coefficients are greatly improved.
2. The accuracy of the parameterization methods of Swinbank (1963) and Idso and Jackson (1969) is worse than the other parameterization methods, because water vapor is not considered. Therefore, they are not incorporated in BMA.
3. The parameterization of Carmona et al. (2014) performs best, whose BIAS, RMSE, and R^2 are −0.11 W/m^2, 20.35 W/m^2, and 0.92, respectively, followed by the parameterization methods of Idso (1981), Prata (1996), Brunt and Sc (1932), and Brutsaert (1975).
4. The accuracy of BMA is close to that of the parameterization method of Carmona et al. (2014) and comparable to that of the parameterization method of Idso (1981).
5. On the whole, a method that can be successfully applied everywhere does not exist; even the five selected parameterization methods and BMA can achieve high accuracy of SDLR estimates. Fox example, the five parameterization methods and BMA all failed over land with the tropical climate type, with high water vapor, and had poor results over forest, wetland, and ice. These methods achieved better results over desert, bare land, cropland, and grass and obtain acceptable accuracies for sites at different elevations, with the exception of the parameterization method of Carmona et al. (2014) over high elevation sites.

Regarding the cloudy skies, SDLR is substantially modified by the cloud. Both clear-sky SDLR and cloud information (e.g., cloud cover) are required to estimate cloud-sky SDLR in the widely used parameterization methods. Based on the conclusions drawn from this study, a cloud-sky SDLR method that can be successfully applied everywhere may also not exist. Thus, comprehensive assessment of mainstream cloud-sky parameterization methods is urgently needed.

Acknowledgements The AmeriFlux data was downloaded from http://asiaflux.yonsei.kr/index.html, the AsiaFlux data was downloaded from https://db.cger.nies.go.jp/asiafluxdb/, the CEOP data was downloaded from http://aan.suiri.tsukuba.ac.jp, the Fluxnet data was downloaded from http://daac.ornl.gov/get_data.shtml, and the SURFRAD data was downloaded from http://www.srrb.noaa.gov, respectively.

Funding information This work was partly supported by the National Natural Science Foundation of China via grant 41771365, the National Key Research and Development Program of China via grant 2016YFA0600101, and the Special Fund for Young Talents of the State Key Laboratory of Remote Sensing Sciences via grant 17ZY-02.

References

Bisht G, Bras RL (2011) Estimation of net radiation from the moderate resolution imaging spectroradiometer over the continental united states. IEEE Trans Geosci Remote Sens 49(6):2448–2462

Brunt D, Sc MAB (1932) Notes on radiation in the atmosphere. I. Q J R Meteorol Soc 58(247):389–420

Brutsaert W (1975) On a derivable formula for long-wave radiation from clear skies. Water Resour Res 11(5):742–744

Carmona F, Rivas R, Caselles C (2014) Estimation of daytime downward longwave radiation under clear and cloudy skies conditions over a sub-humid region. Theor Appl Climatol 115:281–295

Cheng J, Liang S (2016) Global estimates for high spatial resolution clear-sky land surface upwelling longwave radiation from MODIS data. IEEE Trans Geosci Remote Sens 54(7):4115–4129

Crawford TM, Duchon CE (1999) An improved parameterization for estimating effective atmospheric emissivity for use in calculating daytime downwelling longwave radiation. J Appl Meteorol 38(4):474–480

Duarte HF, Dias NL, Maggiotto SR (2006) Assessing daytime downward longwave radiation estimates for clear and cloudy skies in Southern Brazil. Agric Forest Meteorol 139(3–4):171–181

Flerchinger GN, Wei X, Marks D, Sauer TJ, Qiang Y (2009) Comparison of algorithms for incoming atmospheric long-wave radiation. Water Resour Res 45(3):450–455

Gupta SK, Kratz DP, PWS R JR, Wilber AC, Zhang T, Sothcott VE (2010) Improvement of surface longwave flux algorithms used in the CERES processing. J Appl Meteorol Climatol 49:1579–1589

Hoeting HA, Madigan D, Raftery AE, Volinsky CT (1999) Bayesian model averaging: a tutorial. Stat Sci 14(4):382–417

Idso SB (1981) A set of equations for full spectrum and 8- to 14-mm and 10.5- to 12.5-mm thermal radiation from cloudless skies. in *Res*

Idso SB, Jackson RD (1969) Thermal radiation from the atmosphere. J Opt Soc Am 46(7):543–547

Kjaersgaard JH, Plauborg FL, Hansen S (2007) Comparison of models for calculating daytime long-wave irradiance using long term data set. Agric Forest Meteorol 143(1–2):49–63

Kruk NS, Vendrame ÍF, Rocha HRD, Chou SC, Cabral O (2010) Downward longwave radiation estimates for clear and all-sky conditions in the Sertãozinho region of São Paulo, Brazil. Theor Appl Climatol 99(1–2):115–123

Liang S, Wang K, Zhang X, Wild M (2010) Review of estimation of land surface radiation and energy budgets from ground measurements, remote sensing and model simulation. IEEE J Sel Topics Earth Obs Remote Sens 3(3):225–240

Marks D, Dozier J (1979) A clear-sky longwave radiation model for remote alpine areas. Theor Appl Climatol 27(2):159–187

Prata AJ (1996) A new long-wave formula for estimating downward clear-sky radiations at the surface. Q J R Meteorol Soc 122: 1127–1151

Raftery AE, Gneiting T, Balabdaoui F, Polakowski M (2003) Using Bayesian model averaging to calibrate forecast ensembles. Mon Weather Rev 133(5):1155–1174

Rizou M, Nnadi F (2007) Land use feedback on clear sky downward longwave radiation: a land use adapted model. Int J Climatol 27(11):1479–1496

Santos CACD, Silva BBD, Rao TVR, Satyamurty P, Manzi AO (2011) Downward longwave radiation estimates for clear-sky conditions over northeast Brazil. Revista Brasileira De Meteorologia 26(3): 443–450

Schmetz J (1989) Towards a surface radiation climatology: retrieval of downward irradiances from satellites. Atmopsheric Research 23(3–4):287–321

Sugita M, Brutsaert W (1993) Cloud effect in the estimation of instantaneous downward longwave radiation. Water Resour Res 29(3):599–606

Swinbank WC (1963) Long-wave radiation from clear skies. Q J R Meteorol Soc 89:339–348

Wang GY, Chen L (2013) Consistent retrieval methods to estimate land surface shortwave and longwave radiative flux components under clear-sky conditions. Remote Sens Environ 124(61–71)

Wang W, Liang S (2009a) Estimation of high-spatial resolution clear-sky longwave downward and net radiation over land surfaces from MODIS data. Remote Sens Environ 113(4):745–754

Wang K, Liang S (2009b) Global atmospheric downward longwave radiation over land surface under all-sky conditions from 1973 to 2008. J Geophys Res - Atmos 114:D19101. https://doi.org/10.1029/2009JD011800